

*Electronic Supplementary Information (ESI)*

## **Synthesis of Zeolite@Metal Organic Framework Core-Shell**

### **Particles as Bifunctional Catalysts**

Guanghui Zhu, Richard Graver, Laleh Emdadi, Baoyu Liu, Kyo-Yong Choi and Dongxia Liu\*

*Department of Chemical and Biomolecular Engineering, University of Maryland, College Park, MD, 20742*

\*Corresponding author:

Prof. Dongxia Liu

Email: liud@umd.edu

Phone: (+1) 301-405-3522

Fax: (+1) 301-405-0523

## S.1. Experimental

### *SI.1. Synthesis of ZSM-5 zeolite*

ZSM-5 zeolite was hydrothermally synthesized by using the recipe with a composition of  $100\text{SiO}_2:0.5\text{Al}_2\text{O}_3:1\text{NaOH}:36\text{TPAOH}:4000\text{H}_2\text{O}$ , where TPAOH stands for tetrapropylammonium hydroxide (40% in aqueous solution, Alfa Aesar). Typically, 0.0111 g NaOH (97%, Sigma-Aldrich) and 5.075 g 40wt% TPAOH solution were added to 20 g deionized (DI) water. Subsequently, 0.0564 g aluminum isopropoxide (99.99%, Alfa Aesar) and 5.78 g tetraethylorthosilicate (TEOS, 98%, Alfa Aesar) were added to the solution. The as-prepared mixture was allowed to stir vigorously at room temperature for 8 h, followed by 5 days in tumbling Teflon-lined steel autoclaves at 423 K. The product was collected by centrifugation and washed with DI water repeatedly to reduce pH to  $\sim 9$ . Afterwards, the product was dried at 343 K and calcined at 873 K under flowing air ( $150 \text{ mL min}^{-1}$ ) for 6 h. The as-synthesized ZSM-5 was ion exchanged three times using  $1 \text{ mol L}^{-1}$  aqueous  $\text{NH}_4\text{NO}_3$  solution at 353 K for 2 h, and subsequently, collected by centrifugation, washed with DI water for three times, and dried at 343 K overnight. The zeolite sample in its  $\text{NH}_4^+$ -form was treated in flowing air ( $150 \text{ mL min}^{-1}$ ) by increasing the temperature from ambient to 823 K at  $1.5 \text{ K s}^{-1}$  and holding for 4 h to thermally decompose to  $\text{NH}_3$  and  $\text{H}^+$ .

### *SI.2. Synthesis of UiO-66 and ZSM-5@UiO-66*

The synthesis of UiO-66 particles was carried out as follows: 0.106 g  $\text{ZrCl}_4$  (99.9%, Alfa Aesar) and 0.068 g 1,4-benzene-dicarboxylate (BDC, 98%, Alfa Aesar) were dissolved in 24.9 g dimethylformamide (DMF, 99.8%, BDH) in sequence. The solution was transferred to a Teflon-lined stainless steel autoclave and allowed to react at 393 K for 24 h. The product was collected

by centrifugation and washed by dispersing in DMF for 12 h under rigorous magnetic stirring. The DMF washing and centrifugation steps were repeated three times. Afterwards, the sample was dispersed in methanol solvent for 12 h followed by centrifugation in order to remove the DMF solvent. This step was repeated two times. Finally, the sample was dried in a vacuum oven at 423 K overnight. The synthesis of ZSM-5@UiO-66 core-shell composite was performed by using the same procedure as described above except that 0.15 g ZSM-5 particles were added to the UiO-66 synthetic solution prior to the solvothermal crystallization of MOF particles.

### *S1.3. Incorporation of amine ( $-NH_2$ ) groups into ZSM-5@UiO-66*

The incorporation of amine groups into the composites was performed in a 150 mL flask equipped with a reflux condenser and heated in a temperature controlled oil bath under atmospheric pressure and magnetic stirring (500 rpm) conditions. Firstly, 150  $\mu$ L ethylene diamine (99.5%, Sigma-Aldrich) and 90 mL anhydrous toluene (99.5%, BDH) were added into the flask. 1.5g ZSM-5@UiO-66 composite particles were then added to the ethylene diamine/toluene solution. After the suspension was refluxed at 385 K for 12 h, the ZSM-5@UiO-66 particles were collected by centrifugation and washed by dispersing in absolute ethanol. The ethanol washing and centrifugation steps were repeated three times. Finally, the particles were dried in convective oven at 343 K overnight. The as-obtained sample was denoted as ZSM-5@UiO-66-NH<sub>2</sub>.

The ethylene diamine trapped in the micropores of ZSM-5 and UiO-66 was removed by an acid extraction process that was carried out as follows. 0.6 g ZSM-5@UiO-66-NH<sub>2</sub> was dispersed in 100 mL of 0.01 M HCl ethanol solution in a 50 mL flask equipped with a condenser. The mixture was refluxed at 363 K for 3 h. After the acid extraction process, the ZSM-5@UiO-

66-NH<sub>2</sub> particles were collected by centrifugation and washed by dispersing in DI water and absolute ethanol repeatedly. A vacuum oven was utilized to dry the wet sample at 423 K overnight. The as-obtained sample was used for the catalytic cascade reactions.

#### *SI.4. Catalytic reaction over ZSM-5@UiO-66-NH<sub>2</sub>*

The liquid phase catalytic conversion of benzylidene malononitrile from malononitrile and benzaldehyde dimethyl acetal was carried out in a three-necked flask equipped with a reflux condenser. The reactor was heated in a temperature controlled oil bath under atmospheric pressure and magnetic stirring (500 rpm) conditions. In a typical experiment, 20 mL acetonitrile (99.9%, Fisher), 0.0866 g malononitrile (1.31 mmol, 99%, Sigma-Aldrich), 7.5  $\mu$ L DI water, and 0.05 g catalyst (ZSM-5@UiO-66-NH<sub>2</sub>) were added into the flask in sequence. After bubbling the mixture with flowing helium for 0.5 h, the flask was immersed in the oil bath preheated at 353 K. The reaction mixture was maintained for 0.5 h at the required reaction temperature and stirring conditions and then 0.2045 mL of benzaldehyde dimethyl acetal (1.36 mmol) was added. This moment of addition was taken as the initial reaction time. Liquid samples were withdrawn at regular intervals and analyzed by the gas chromatograph (Agilent 7890A) equipped with a methyl-siloxane capillary column (HP-1, 50.0 m x 320  $\mu$ m x 0.52  $\mu$ m) connected to a flame ionization detector. The influence of external mass transfer limitations on the reaction rates was ruled out by running the reactions at a high enough stirring speed (500 rpm), showing a further increase in the stirring speed did not enhance the reaction rate. The reactant mixture without addition of catalyst showed no conversion of any reactant under the investigated reaction conditions.

### *S1.5. Materials characterization*

The crystalline phase of the samples was determined by X-Ray powder diffraction (XRD) using Bruker D8 Advance Lynx Powder Diffractometer. The integration time was 0.3 hours and the step size was 0.032 degrees/second. The morphology and elemental analysis of the samples were obtained by a scanning electron microscope (SEM, Hitachi SU-70) equipped with an energy dispersive X-ray (EDX) spectrometer. Transmission electron microscopy (TEM) images were recorded on a JEM 2100 LaB6 microscope at an accelerating voltage of 200 KV. Nitrogen and argon adsorption-desorption measurements were carried out at 77 K and 87 K on an Autosorb-iQ analyzer (Quantachrome Instruments), respectively. Prior to the nitrogen and argon measurements, samples were degassed at 423 K overnight. The FT-IR spectrum was recorded with a spectrometer (Nicolet Magna-IR 560) in the range of 4000 - 400  $\text{cm}^{-1}$ . Each sample was measured with 128 scans at an effective resolution of 4  $\text{cm}^{-1}$ . The thermogravimetric analysis (TGA) was conducted using a thermogravimetric analyzer (TGA 2950, TA Instruments) under a mixed air and  $\text{N}_2$  flow (100  $\text{mL min}^{-1}$ , 60% air and 40%  $\text{N}_2$ ) with a heating rate of 5  $\text{K min}^{-1}$  from 298 K to 1073 K. Si and Al contents of the zeolite sample were determined by inductively coupled plasma optical emission spectroscopy (ICP-OES) using Optima 4300 DV instrument (Perkin-Elmer). The measured Si/Al ratio of the sample was 115.

### **S.2 Assessment of elemental composition by EDX spectroscopy**

The elemental composition of the prepared ZSM-5 core and ZSM-5@UiO-66 core-shell particles was verified with EDX spectroscopy, and the results are shown in Fig. S1. The EDX spectrum of the ZSM-5 particles (Fig. S1 (A)) is comprised of Si, Al, and O peaks, consistent with the composition of ZSM-5 zeolites. In comparison with ZSM-5, the EDX spectrum of

ZSM-5@UiO-66 composite (Fig. S1 (B)) contains Zr peak besides the element peaks shown in Fig. S1 (A). The presence of Zr peak indicates the existence of UiO-66 in the composite structure. The C peak in Fig. S1 (A) is from the carbon tape used for sample preparation in SEM/EDX characterization. Due to the composition of UiO-66 ( $Zr_6O_4(OH)_4(O_2C-C_6H_4-CO_2)_6$ ), the C peak in Fig. S1 (B) comes from both carbon tape on the sample stage and carbon in UiO-66.

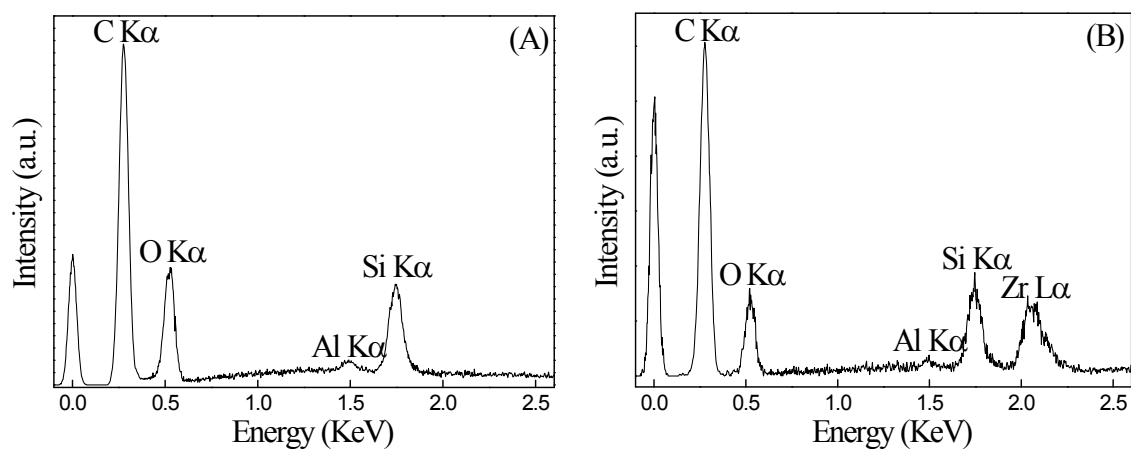


**Figure S1.** EDX spectra of as-synthesized (A) ZSM-5 and (B) ZSM-5@UiO-66 core-shell composite particles.

### S.3 Textural property analysis ( $N_2$ isotherms and Pore size analysis from Ar isotherm)

$N_2$  adsorption-desorption measurement was conducted to determine the textural properties of ZSM-5, UiO-66, ZSM-5@UiO-66 and ZSM-5@UiO-66-NH<sub>2</sub>, respectively. Figure S2 shows the  $N_2$  isotherms of these samples. The  $N_2$  uptake of ZSM-5@UiO-66 and ZSM-5@UiO-66-NH<sub>2</sub> is lower than UiO-66 and higher than ZSM-5, consistent with the Ar uptake of these samples. The textural properties of these samples were included in Table S1. The Brunauer–Emmett–Teller (BET) surface area, total pore volume, and micropore volume are all in the order of ZSM-5 < ZSM-5@UiO-66-NH<sub>2</sub> < ZSM-5@UiO-66 < UiO-66, illustrating that the zeolite@MOF composite consists of topology features of both porous materials. Additionally, the inclusion of

amino groups in the composite did not block the micropores of either zeolite or MOF significantly.

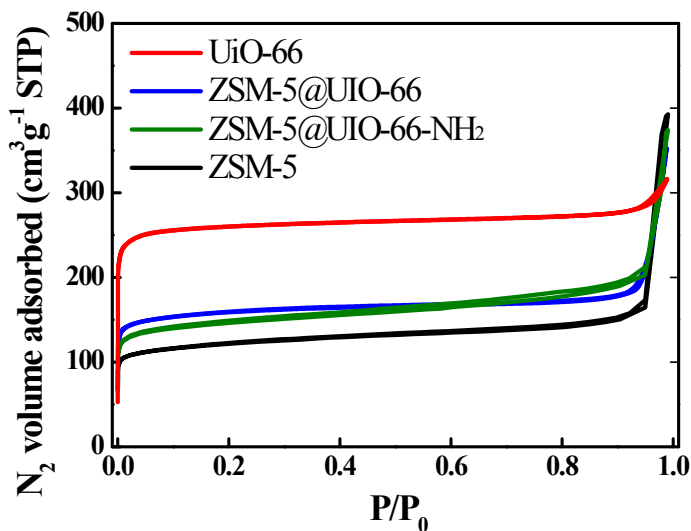


**Figure S2.**  $N_2$  adsorption-desorption isotherms of ZSM-5, UiO-66, ZSM-5@UiO-66, and ZSM-5@UiO-66-NH<sub>2</sub>, respectively.

**Table S1.** Textural properties of UiO-66, ZSM-5, ZSM-5@UiO-66, ZSM-5@UiO-66-NH<sub>2</sub>, analyzed from  $N_2$  isotherms.

Samples	$S_{\text{micro}}^a$ [ $m^2 g^{-1}$ ]	$V_{\text{micro}}^a$ [ $cm^3 g^{-1}$ ]	$V_{\text{total}}^b$ [ $cm^3 g^{-1}$ ]	$S_{\text{BET}}^c$ [ $m^2 g^{-1}$ ]
UiO-66	1002	0.38	0.43	1048
ZSM-5	390	0.15	0.25	466
ZSM-5@UiO-66	570	0.22	0.29	621
ZSM-5@UiO-66-NH <sub>2</sub>	466	0.19	0.31	564

<sup>a</sup> Determined from *t*-plot method. <sup>b</sup> Total pore volume calculated at  $P/P_0=0.95$ . <sup>c</sup> Determined from multi-point BET method.

Non-local density functional theory (NLDFT) pore size analysis in Fig. 3(B) in the main text shows that ZSM-5 has a micropore size of 7.1 Å, larger than the typical micropore size (5.2 Å) of ZSM-5. The analysis was derived from the adsorption branch of Ar isotherms on the basis of

spherical/cylindrical pore model. To verify the influences of pore model selected in the analysis on the micropore sizes of ZSM-5 and UiO-66 materials, the Ar adsorption branches were further analyzed on the basis of a cylindrical pore model, and the resultant pore size distributions are shown in Fig. S3. ZSM-5 has a typical pore size of  $\sim 5.2 \text{ \AA}$ , while UiO-66 has a micropore size of  $\sim 6.1 \text{ \AA}$  and  $\sim 5.0 \text{ \AA}$  (a shoulder next to the peak), corresponding to its tetrahedral cages and octahedral cages, respectively. These results also demonstrate that ZSM-5@UiO-66-NH<sub>2</sub> and ZSM-5@UiO-66 is comprised of dual micropore systems.

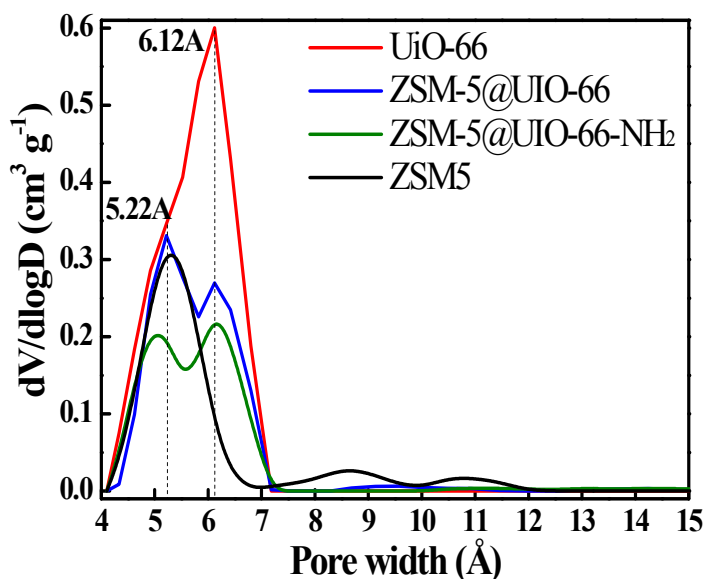


**Fig. S3** NLDFT pore-size distribution curves obtained from the adsorption branch of Ar isotherms on the basis of a cylindrical pore model.

### S.5 Thermogravimetric analysis of ZSM-5@UiO-66

The TGA was performed to study the thermal stability and the mass fractions of UiO-66 and ZSM-5 in the composite materials. Fig. S4 shows the TGA curves of ZSM-5, UiO-66, ZSM-5@UiO-66 and ZSM-5@UiO-66-NH<sub>2</sub>, respectively. The weight loss in the proton-form ZSM-5 is 3.3 wt%, due to the loss of moisture adsorbed in the zeolite. UiO-66 showed the weight loss in



two stages with increasing temperature. The first stage of weight loss happened below 600 K, which resulted from the moisture desorption from the UiO-66 sample. The second stage of weight loss stayed between 690 K and 800 K, which is mainly due to the decomposition of MOF structure. Clearly, UiO-66 is stable at temperature below  $\sim 650$  K in air. The trend of weight loss in ZSM-5@UiO-66 and ZSM-5@UiO-66-NH<sub>2</sub> is similar to that of UiO-66, but the total weight loss is 22.8 wt% compared to 56.2 wt% in UiO-66. The composition of UiO-66 and ZSM-5 in the composite particles therefore can be estimated from these TGA curves. The calculation showed that the composite contains 41.4 wt% UiO-66.

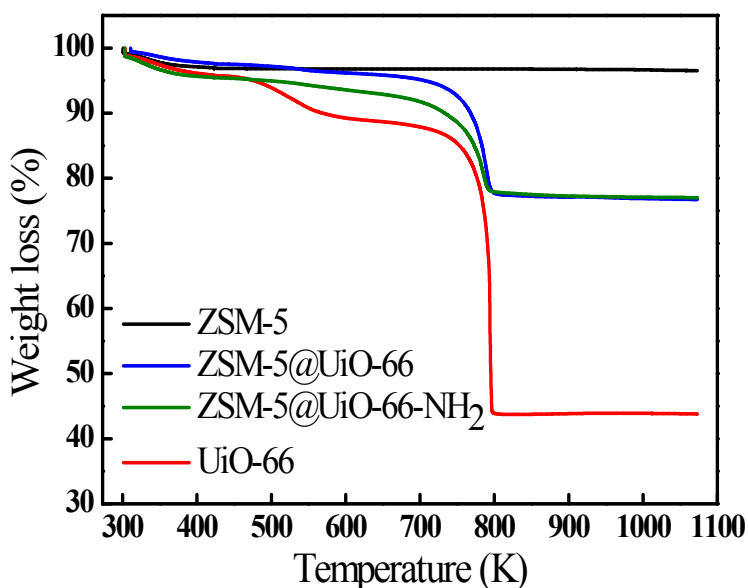


**Fig. S4** TGA curves of ZSM-5, UiO-66, ZSM-5@UiO-66 and ZSM-5@UiO-66-NH<sub>2</sub>, respectively.

### S.6 Cascade reaction over bare ZSM-5 or UiO-66-NH<sub>2</sub>, and physical mixture ZSM-5 and UiO-66-NH<sub>2</sub> catalysts

In order to examine the acid-base functionality of ZSM-5@UiO-66-NH<sub>2</sub> composite

catalyst, the cascade reaction was studied over proton-form ZSM-5 and UiO-66-NH<sub>2</sub>, respectively. It should be noted that UiO-66 is prepared by using the procedure for ZSM-5@UiO-66 described in Section S1.3. Fig. S5(A) illustrates that ZSM-5 itself enabled catalytic reaction for conversion of benzaldehyde dimethyl acetal to benzaldehyde since intermediate product benzaldehyde is the only observed product. UiO-66-NH<sub>2</sub>, however, showed almost negligible activity for either reaction (Fig. S5(B)). The absence of acid sites of ZSM-5 or basic sites of UiO-66 cannot enable the cascade reactions. These results further confirm the bifunctionality of ZSM-5@UiO-66-NH<sub>2</sub> composite catalyst.

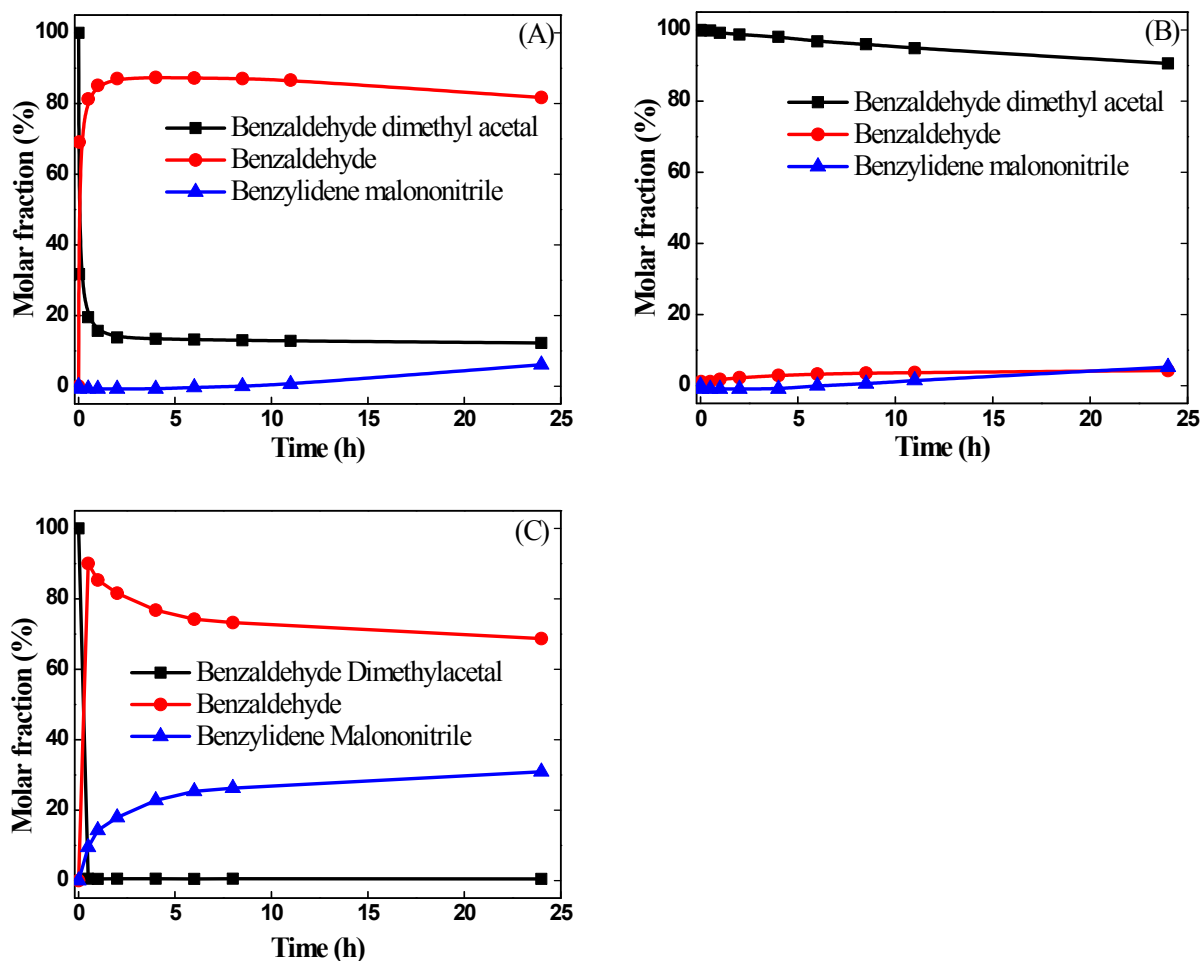


**Fig. S5** Results of catalytic cascade reaction over ZSM-5 (A), UiO-66-NH<sub>2</sub> (B), and physical mixture of ZSM-5 and UiO-66-NH<sub>2</sub> in the same weight ratio as ZSM-5@UiO-66-NH<sub>2</sub> catalysts (C), respectively.

The cascade reaction was also conducted over the physical mixture of ZSM-5 and UiO-66-NH<sub>2</sub> catalysts. The weight ratios of ZSM-5 and UiO-66-NH<sub>2</sub> in the physical mixture were the same as those in the ZSM-5@UiO-66-NH<sub>2</sub> core-shell catalyst. Fig. S5(C) shows that the reactant, benzaldehyde dimethyl acetal, is consumed entirely to form benzyldehyde intermediate in the very early stage of the reaction. The final product, benzylidene malononitrile, however, forms slowly with the reaction time. In comparison with the integrated core-shell structured catalysts, the formation rate of the benzylidene malononitrile over the physical mixture of ZSM-5 and UiO-66-NH<sub>2</sub> catalysts is lower. The lower reaction rate might be caused by the slow mass transport in the UiO-66-NH<sub>2</sub> since it has larger particle sizes compared to UiO-66-NH<sub>2</sub> in the composite ZSM-5@UiO-66-NH<sub>2</sub> particles. A synergy between the acid site in ZSM-5 and basic site in UiO-66-NH<sub>2</sub> may also play a role in enhancing the formation rate of the final product in the cascade reaction.

To investigate the reusability of the composite catalysts, the spent ZSM-5@UiO-66-NH<sub>2</sub> catalyst was collected by centrifugation and dried in a vacuum oven at 423 K overnight, and then reused in the cascade reaction. No obvious drop in catalytic activity was observed, which indicates the composite catalyst has a good stability in the studied reaction conditions.